Transactions, SMiRT-22
San Francisco, California, USA - August 18-23, 2013
Division I

MODELING OF STEAM GENERATOR TUBE RUPTURE USING EXTENDED FINITE ELEMENT METHOD

Subhasish Mohanty[1], Saurin Majumdar[2], and Ken Natesan[3]

[1]Mechanical Engineer, Nuclear Engineering Division, Argonne National Laboratory, Lemont, IL (smohanty@anl.gov)
[2]Senior Mechanical Engineer, Nuclear Engineering Division, Argonne National Laboratory, Lemont, IL
[3]Distingushed Fellow & Section Manager, Nuclear Engineering Division, Argonne National Laboratory, Lemont, IL

ABSTRACT

A steam generator (SG) is an important component of any pressurized water reactor (PWR) system. Steam generator tubes represent a primary pressure boundary whose integrity is vital to the safe operation of the reactor. SG tubes may rupture due to propagation of a crack that might have been created by mechanisms such as stress corrosion cracking, fatigue, etc. It is important to estimate the rupture pressures of cracked tubes for safety boundary integrity evaluation of PWRs. The present paper discusses the use of extended finite element method to estimate the rupture pressures of SG tubes with an existing flaw. Elastic-plastic finite element models were developed for Alloy 600 SG tubes with different crack shapes. The simulation results were validated by experimental results generated under the United States Nuclear Regulatory Commission (US-NRC)-sponsored SG tube integrity program (SGTIP) conducted at Argonne National Laboratory (ANL). It was found that there is a good correlation between extended finite element model results and experimental results.

INTRODUCTION

In the United States, long-term sustainability of light water reactors (LWRs) is increasingly becoming an important issue because many of the operating reactors have either reached or are close to reaching their design life of 30-40 years. For economical reasons, it is desirable to keep these reactors operating for longer duration, say up to 60-80 years (DOE report, 2010). However, stress corrosion cracking and associated structural integrity issues are a major concern for long-term sustainability of LWRs (Shah and Macdonald, 1993 and Busby, 2012). Under the auspices of the Department of Energy (DOE)'s light water reactor sustainability (LWRS) research program, ANL is currently investigating stress corrosion cracking and fatigue related issues in reactor coolants system (RCS) piping and tubing material. Steam generator tubes constitute a critical part of the primary coolant pressure boundary. These tubes often crack by stress corrosion cracking (SCC) and fatigue. These cracks may initiate from either the inner or the outer surface of the tube, depending on the environmental exposure and stress levels. Initially, these cracks are part-through-wall (PTW) but can eventually become 100% through-wall (TW) cracks either due to normal operating loading conditions or due to transient pressure loading during design-basis or severe accident conditions. To guard against catastrophic failure, the Nuclear Regulatory Commission (NRC) requires utilities to conduct periodic in-service inspections (ISI) to detect cracks and, if detected, take proper remedial actions in order to ensure and demonstrate, by calculations or in-situ pressure tests, that adequate safety margins are maintained against burst and leakage throughout the component's lifetime during normal operation and various accident scenarios. Therefore, it is essential to be able to estimate the ligament rupture/burst pressure of a tube with a PTW/TW crack reliably. In general, the tube rupture pressure or time to failure of a tube are estimated using extensive laboratory tests (Bakhtiari, et. al., 2003) or by combined use of empirical methods (Majumdar, 1993) and finite element (FE) techniques (Majumdar, 2001, Lee, et. al., 2001, Abou-Hanna, et. al., 2004, Moon et.al, 2007, and Chang, et. al. 2007). Tube rupture modeling by conventional finite element method (FEM) is difficult, particularly for

modeling continuous crack initiation and crack propagation. The conventional FEM requires remeshing of the finite element domain after each crack propagation increment and requires that the crack path be known beforehand. In reality, the crack path is not known a-priori. An efficient crack propagation modeling requires the crack path to be solution dependent or automatic. In conventional FEM, at each time interval during which the crack grows, the element boundary has to be aligned along the crack path, which may not always be the case in practice. Further, conventional FEM often runs into numerical difficulties while modeling discontinuities, such as cracks. All of the above-mentioned limitations have restricted the use of conventional FEM for modeling a moving crack tip.

The recent advancement of the extended finite element method (XFEM) has made it possible to model moving cracks efficiently. The development of XFEM was first linked to the work of Babuska, 1994 and Melenk and Babuska, 1996. They proposed the partition of unity method (PUM), which involved the use of local enrichment functions to model cracks. This procedure avoids singularity problems associated with discontinuities in conventional FEM. Also, the development of the level set method (LSM) by Sethian, 1999 has made it easier to model moving interfaces or shapes, such as cracks. The LSM has made it possible to perform numerical computations involving curves and surfaces on a fixed Cartesian grid without having to parameterize the bulk material or object. Belytschko and Black, 1999 first extended the concept of PUM and LSM to conventional FEM for solving linear elastic fracture mechanics problems. The resulting method is popularly known as the extended finite element method or XFEM. The XFEM method was further improved by many other researchers (Sukumar, et. al., 2000, Shi et. al. 2010) and has recently been implemented in commercially available software, such as ABAQUS. In the present work, the use of XFEM through ABAQUS is explored by modeling crack initiation and propagation in steam generator tubes with existing crack. The results were compared with the experimental results available under ANL's SGTIP sponsored by US-NRC (Bakhtiari, et. al., 2003). The details of the model and results are briefly discussed in the following sections.

THEORETICAL BACKGROUND

Extended Finite Element Method: Generic Theoretical Background

In the generic XFEM framework (Belytschko and Black, 1999, Sukumar, et. al., 2000, Shi et. al. 2010), the displacement field in a finite element crack domain can be expressed as

$$\begin{aligned} u &= \sum_{i}^{N} N_i(x) q_i + enriched \quad function \\ &= \sum_{i=1}^{N} N_i(x) q_i + \sum_{i=1}^{N} N_i(x) H(x) a_i + \sum_{i=1}^{N} N_i(x) \sum_{\alpha=1}^{4} F_\alpha b_i^\alpha \\ &= \sum_{i=1}^{N} N_i(x) \left[q_i + H(x) a_i + \sum_{\alpha=1}^{4} F_\alpha b_i^\alpha \right] \end{aligned} \tag{1}$$

where $N_i(x)$ and q_i are, respectively, the usual nodal shape functions and nodal degree-of-freedom (DOF) vector used in conventional FEM and associated with the continuous part of the finite element model; $H(x)$ and a_i are, respectively, the Heaviside function and nodal-enriched DOFs associated with the cracked geometry; and F_α and b_i^α are, respectively, the additional asymptotic crack tip functions and the associated enriched-nodal DOFs. The Heaviside function $H(x)$ can be given as

$$H(x) = \begin{cases} +1 & x \ above \ the \ crack \ surface \\ -1 & x \ below \ the \ crack \ surface \end{cases} \tag{2}$$

The asymptotic crack tip functions F_α can be given as

$$F_\alpha(x) = \left\{ \sqrt{r}\sin(\frac{\theta}{2}) \ , \quad \sqrt{r}\cos(\frac{\theta}{2}) \ , \quad \sqrt{r}\sin(\theta)\sin(\frac{\theta}{2}) \ , \quad \sqrt{r}\sin(\theta)\cos(\frac{\theta}{2}) \right\} \tag{3}$$

where (r,θ) is the polar coordinate system with its origin at the crack tip.

XFEM Modeling Through ABAQUS

In the present work, commercially available ABAQUS based extended finite element technique is used to model the initiation and propagation of moving cracks in steam generator tubes. For simplicity in modeling moving cracks, the current version of ABAQUS does not allow consideration of the displacement field associated with the asymptotic crack tip functions given in Eq. (1). Hence the total displacement field considered for modeling a moving crack in the present work is as follows:

$$\begin{aligned} u &= \sum_i^N N_i(x) q_i + enriched \quad function \\ &= \sum_{i=1}^N N_i(x) q_i + \sum_{i=1}^N N_i(x) H(x) a_i = \sum_{i=1}^N N_i(x) \left[\ q_i + H(x) a_i \right] \end{aligned} \tag{4}$$

RESULTS AND ANALYSIS

The above discussed XFEM technique was used to model crack initiation and propagation in steam generator (SG) tubes under pressure transients at room temperature. The results are compared with the experimental data obtained from the NRC-sponsored SG tube integrity experiments conducted at ANL. Multiple Alloy 600 SG tubes were tested under different pressure conditions, and the details of these tests can be found in NUREG/CR-6804 (NRC report, 2003). In the present work, only a few prototypical cases are considered to verify the capability of the XFEM modeling techniques. The details of the model and results are discussed below.

In real nuclear plants, SG tubes containing preexisting SCC cracks may start to grow due to a pressure transient when the internal pressure reaches a critical value. These cracks have highly complex geometry which is difficult to model. Therefore, the tests were conducted on well-defined rectangular notches which are typically much wider (0.1-0.3mm) than SCCs. However, in the FEAs, the notches were modeled as sharp cracks. In the first case, SG tube models were developed with a single preexisting PTW axial crack from the outer diameter (OD) surface. The tubes had an OD of 22.2 mm (7/8 in.), and a thickness of 1.27 mm and were made from Alloy 600 material. The material properties considered for the present FEM are given in Table 1, and the stress-strain curve is shown in Figure 1. Three-dimensional brick elements were used to model the tube. The initial crack was modeled as a shell or planar geometry and superimposed on the tube geometry. A typical FEM of an SG tube is shown in Figure 2. The model includes a part-through-wall OD axial crack with length of 6.35 mm and a ratio for the crack depth to tube wall thickness (a/h) of 75%. In the FEM, the geometric and force boundary conditions are applied such that they are equivalent to the experimental boundary conditions. In the NRC-sponsored SG tube

integrity experiments, one end of the SG tube was fixed to the compressed air flow path, whereas the other end was plugged to help build up the pressure inside the tube. As in the experiment conditions, the FEM model inner surface was subjected to an increasing pressure. In addition, an equivalent longitudinal pressure applied to the end plug was used to simulate the far-field biaxial stress field. Crack initiation and propagation were simulated for an increasing applied internal pressure. Note that the propagation of the initial crack does not occur immediately after the pressurization starts. The crack may start to grow only after a critical pressure is reached.

Table 1 Room-temperature material properties for Alloy 600

Elastic modulus (GPa)	200
Poisson's ratio	0.3
Yield strength σ_y (MPa)	296
Ultimate strength σ_u (MPa)	684
Critical principal stress in Eq. (8) $\sigma_{cr}^{p} = 0.5(\sigma_y + \sigma_u)$	490
Critical fracture energy G_{cr} (kJ/m^2) in Eq. (10)	415

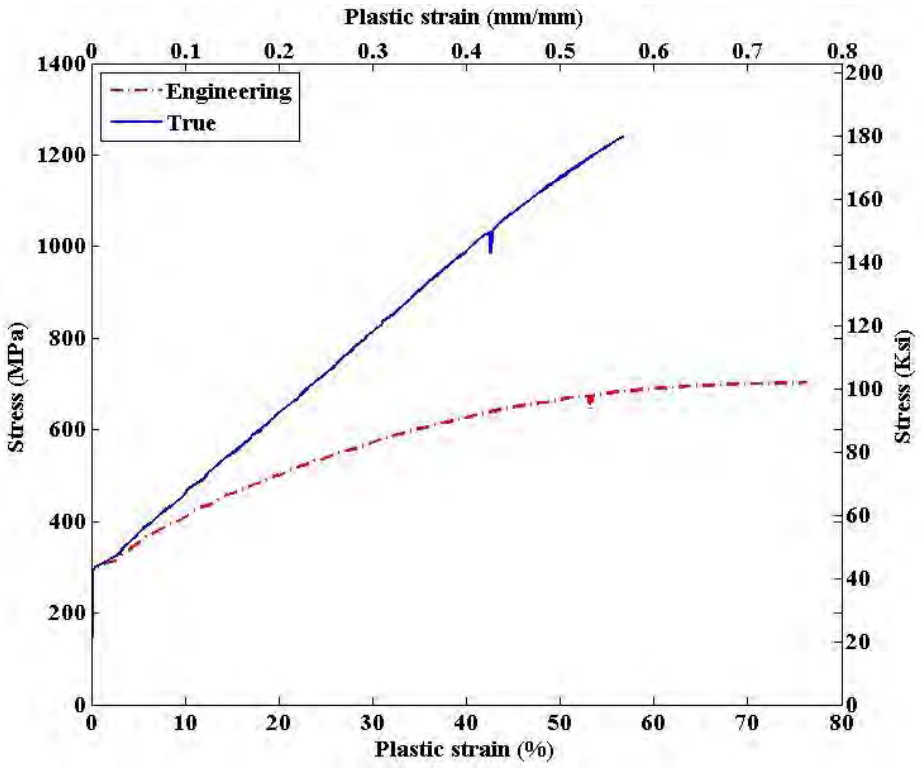

Figure 1 Room-temperature stress-strain curves for Alloy 600

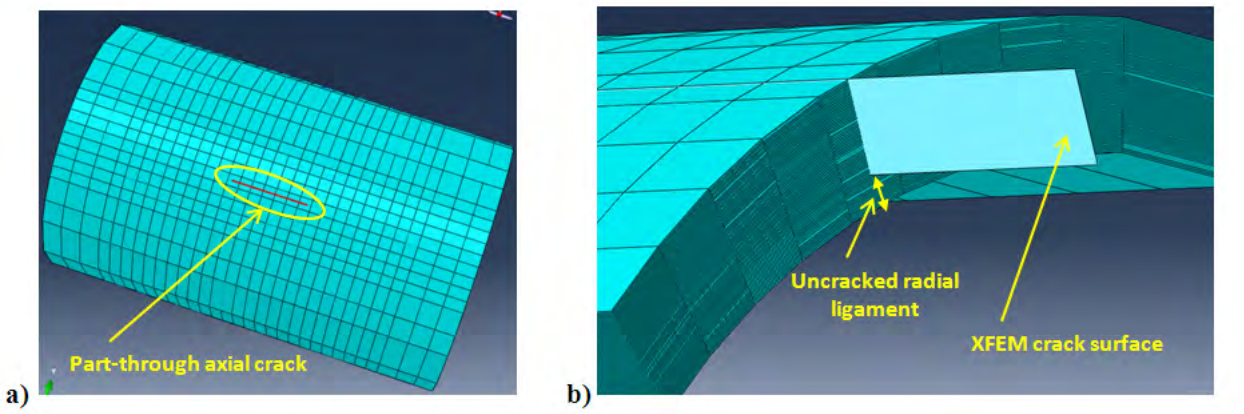

Figure 2 Typical FEM model of a 22.2-mm (7/8-in.) OD tube with an initial crack length of 6.35 mm and crack depth to wall thickness ratio of 75%: (a) OD surface and (b) cut section of the cross section

In the XFEM model, the critical pressure at which the crack begins to grow can be estimated from the solution-dependent maximum principal stress when it equals or exceeds the limiting critical principal stress σ_{cr}^{p} , as given in Table 1. In all the XFEM models discussed in this work, σ_{cr}^{p} is assumed to be the material flow stress which can be approximated as $\sigma_{cr}^{p} = 0.5(\sigma_y + \sigma_u)$. The predicted ligament rupture and final burst pressures based on this assumption match the corresponding experimental values reasonably well. Note that in the experiment, the crack after initiation did not arrest but continued to propagate unstably until full ligament rupture (but before burst). The details of the findings are discussed further below.

For the FEM model shown in Fig. 2, the maximum principal stress distribution at an applied pressure of 24.66 MPa is shown in Fig. 3. The simulation results indicate that the crack starts to propagate along the radial or wall thickness direction at this pressure. They also indicate that the maximum principal stress at the crack tip element exceeds the limiting principal stress (σ_{cr}^{p}) of 490 MPa (Table 1). After initiation, the crack grows further in the radial direction (along the thickness) and ruptures the last ligament in the inner diameter (ID) surface. The corresponding applied pressure is referred to here as "ligament rupture pressure." After the ID ligament ruptures, the crack remains stable and grows in the axial direction unstably only with increasing pressure until the FEM calculation fails to converge because of issues associated with large plastic deformation. The corresponding applied internal pressure is referred to as the "burst pressure." For the FEM model shown in Fig. 2, the estimated ID ligament rupture and burst pressure were found to be 37.73 MPa and 40.01 MPa, respectively. The corresponding experimental values were reported as 36.5 and 41.2 MPa, respectively, showing a good correlation between the XFEM model and experimental results. Figures 4a and 4b show the corresponding OD surface shape at the ligament rupture pressure and burst pressure, respectively. The experimental specimen after bursting, shown in Fig. 5, has a geometry similar to the FEM-predicted shape (Figure 4b). Figure 6 shows the time-dependent (or applied pressure-dependent) crack opening displacement (COD) at the OD and ID surface. It shows that, although the OD COD is larger than the ID COD, both increases unstably after the ID ligament rupture. Figure 7 shows the estimated equivalent plastic strain with respect to applied pressure at a radial crack-tip element (in front of the initial crack) and at a central ID ligament element. Figures 6 and 7 both show that the COD and the maximum equivalent plastic strain behave in a similar manner with increasing pressure. In addition to the above-mentioned model, additional tube models were developed

parametrically with different initial crack shapes. Some of these results are depicted in Figure 8. For example, Figure 8 shows the radial crack initiation pressure and ID ligament rupture pressure as functions of crack depth to thickness ratio (a/h) keeping the length of the crack same (6.35mm) for all cases. It is seen that as a/h increases, the corresponding radial crack initiation and ID ligament rupture pressures decrease non-linearly.

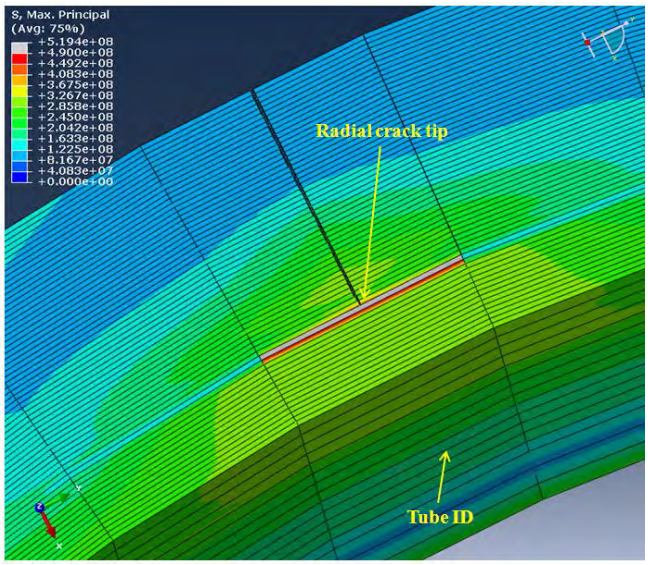

Figure 3 Maximum principal stress distribution upon exceeding the critical principal stress σ_{cr}^{p} just before the crack initiation or cracking of the crack-tip element in front of initial crack in radial direction

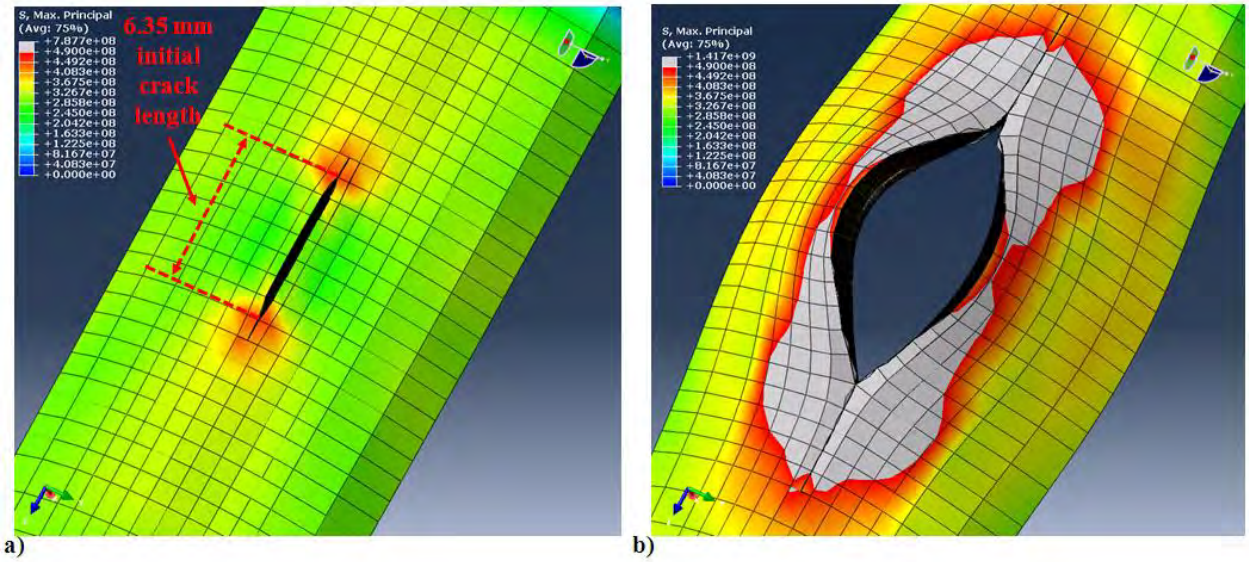

Figure 4 Shape of the OD surface and maximum principal stress distribution for the model shown in Fig. 2 at (a) ID ligament rupture pressure (37.5 MPa) and (b) final burst pressure (40.01 MPa)

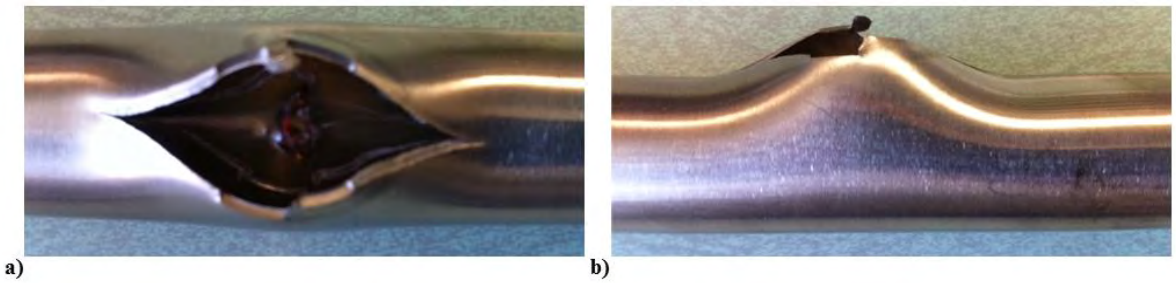

Figure 5 After burst shape of a typical 22.2-mm diameter tube with 6.35 mm initial notch: (a) top view and (b) side view

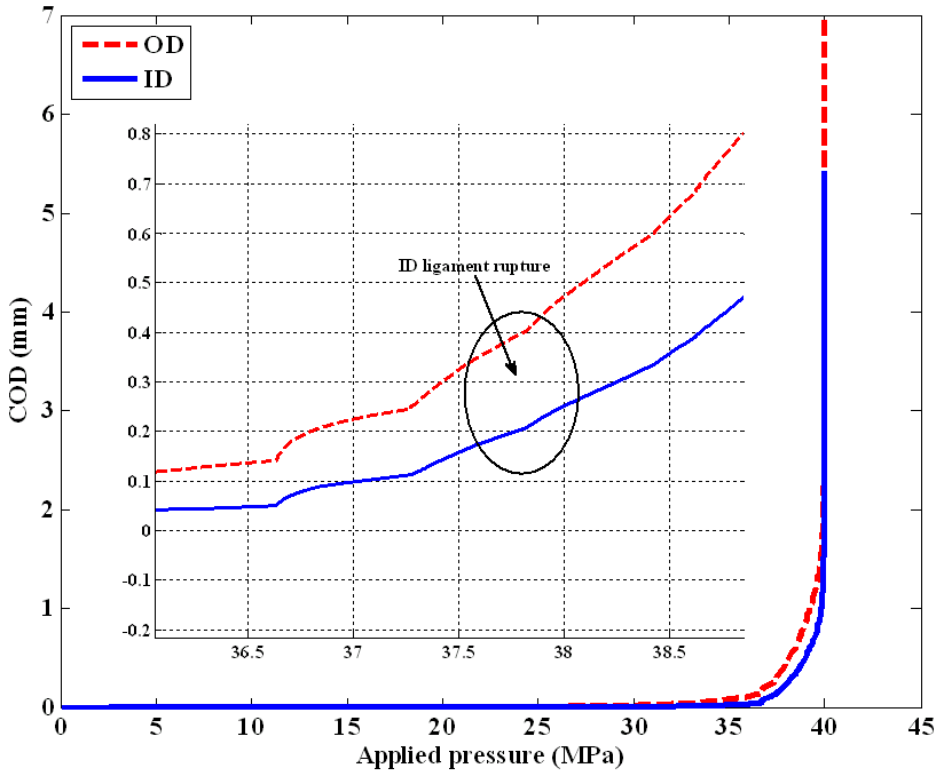

Figure 6 Estimated COD with respect to applied pressure at the OD and ID surface of the 22.2-mm OD tube

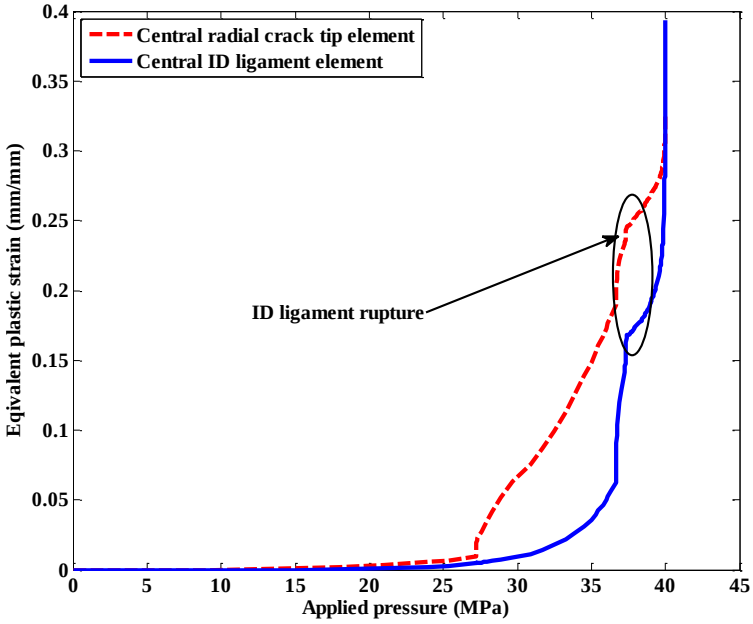

Figure 7 Estimated equivalent plastic strain with respect to applied pressure at radial crack-tip element (in front of the initial crack) and central ID ligament element of the 22.2-mm OD tube

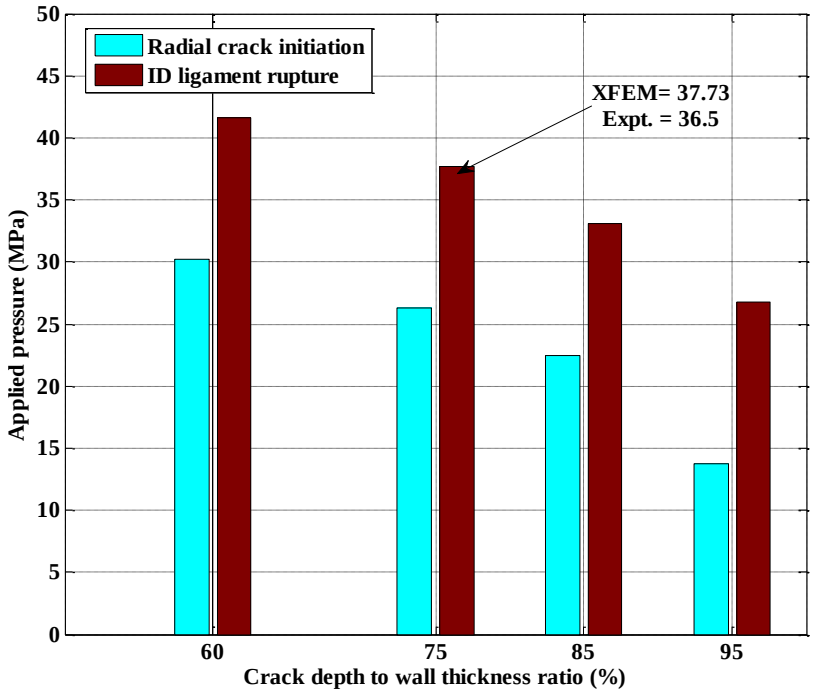

Figure 8 Radial crack initiation pressure and ID ligament rupture pressure with respect to different ratios of initial crack depth to wall thickness, with keeping the length of the crack same (6.35mm) for all cases

CONCLUSION

Multiple XFEM models were developed to predict crack initiation and propagation in Alloy 600 SG tubes with persisting crack. The results are compared with the experimental results available from the NRC-supported tube integrity program and conducted at ANL. The XFEM predicted rupture and burst pressure results agreed well with available experiment results at room temperature. This exercise shows that the XFEM technique can effectively be used to model propagating cracks until SG tube rupture under design-basis accident conditions. A similar technique may be useful to model stress corrosion cracking and fatigue cracks, which are some of our future tasks.

Acknowledgements: This research was sponsored by the U.S. Department of Energy, Office of Nuclear Energy, for the Light Water Reactor Sustainability Research and Development effort, under the program manager Dr. Jeremy Busby. Test results from the US-NRC-sponsored SGTIP program were used to validate the finite element model results.

REFERENCE

1. DOE Report, 2010, Nuclear energy research and development roadmap: Report to congress.
2. Busby, J.T., 2012. Light Water Reactor Sustainability Program Materials Aging and Degradation Pathway Technical Program Plan, ORNL/LTR-2012/327, Oak Ridge National Laboratory, Oak Ridge, TN.
3. Shah, V.N., and Macdonald, P.E., 1993. Aging and life extension of major light water reactor components, Elsevier Press.
4. Bakhtiari, S., Kasza, K. E., Kupperman, D. S., Majumdar, S., Park, J. Y., Shack, W. J., Diercks, D. R., 2003, Second U.S. Nuclear Regulatory Commission International Steam Generator Tube Integrity Research Program – Final Project Summary Report, NUREG/CR-6804 (ANL-02/28)
5. Majumdar, S., 1999, "Prediction of structural integrity of steam generator tubes under severe accident conditions", Nuclear Engineering and Design, Vol-1941999, pp. 31–55.
6. Majumdar, 2001, Structural analysis of electro sleeved tubes under severe accident transients, Nuclear Engineering and Design, Vol. 208, pp. 167–179.
7. Lee, J.H., Park, Y.W., Song, M.H., Kim, Y.J., Moon, S.I., 2001, "Determination of equivalent single crack based on coalescence criterion of collinear axial cracks", Nuclear Engineering and Design, Vol. 205, pp. 1–11.
8. Abou-Hanna, J., McGreevy, T. E., Majumdar, S., 2004, "Prediction of crack coalescence of steam generator tubes in nuclear power plants", Nuclear Engineering and Design, Vol.229, pp. 175–187
9. Moon, S.I., Chang, Y.S., Kim, Y.J., Lee, J.H., Park, Y.W., Song, M.H., 2007, "Determination of failure pressure for tubes with two non-aligned axial through-wall cracks", International Journal of Fracture, Vol. 144, pp. 91–101
10. Chang, Y.S., Huh, N.S., Kim, Y.J., Lee, J.H., Choi, Y.H., 2007, "Coalescence evaluation of collinear axial through-wall cracks in steam generator tubes", Nuclear Engineering and Design,

Vol. 237, pp. 1460–1467

11. Babuska, I., Caloz, G., and Osborn, J., 1994, "Special finite element methods for a class of second order elliptic problems with rough coefficients", SIAM Journal on Numerical Analysis, Vol. 31, pp. 945–981.
12. Melenk, J., and Babuska, I., 1996, "The partition of unity finite element method: Basic theory and applications", Computer Methods in Applied Mechanics and Engineering, Vol. 39, pp.289-314.
13. Sethian, James A., 1999, Level Set Methods and Fast Marching Methods: Evolving Interfaces in Computational Geometry, Fluid Mechanics, Computer Vision, and Materials Science, Cambridge: Cambridge University Press.
14. Belytschko, T., and T. Black, 1999, "Elastic crack growth in finite elements with minimal remeshing", International Journal for Numerical Methods in Engineering, Vol. 45, pp. 601-620.
15. Sukumar, N., Moes, N., Moran, B., and Belytschko, T., 2000, "Extended finite element method for three-dimensional crack modeling", International Journal for Numerical Methods in Engineering, Vol. 48 (11), pp. 1549–1570.
16. Shi, J., Chopp, D., Lua, J., Sukumar, N., Belytschko. T., 2010, "ABAQUS implementation of extended finite element method using a level set representation for three-dimensional fatigue crack growth and life predictions", Engineering Fracture Mechanics, Vol. 77, pp. 2840-2863.
17. ABAQUS 6.11 User Manual, 2011, Dassault Systèmes Simulia Corp.

MODELING OF STEAM GENERATOR TUBE RUPTURE USING EXTENDED FINITE ELEMENT METHOD

Subhasish Mohanty[1], Saurin Majumdar[2], and Ken Natesan[3]

[1]Mechanical Engineer, Nuclear Engineering Division, Argonne National Laboratory, Lemont, IL (smohanty@anl.gov)
[2]Senior Mechanical Engineer, Nuclear Engineering Division, Argonne National Laboratory, Lemont, IL
[3]Distingushed Fellow & Section Manager, Nuclear Engineering Division, Argonne National Laboratory, Lemont, IL

May 2013

Paper submitted to 22nd Structural Mechanics in Reactor Technology (SMiRT-22) conference to be held during 18-23 August 2013, at San Francisco, USA

*Work supported by U.S. DOE under Light Water Reactor Sustainability Program.